

Extension of Experimental Statistical Energy Analysis to Structural Vibration with Low Modal Density

Ikeda, Kazumasa¹

DENSO CORPORATION

1-1 Showa-cho, Kariya, Aichi 448-8661, Japan

Department of Mechanical Engineering, Kanagawa University

3-27-1 Rokkakubashi, Kanagawa-ku, Yokohama, Kanagawa 221-8686, Japan

Yamazaki, Toru²

Department of Mechanical Engineering, Kanagawa University

3-27-1 Rokkakubashi, Kanagawa-ku, Yokohama, Kanagawa 221-8686, Japan

ABSTRACT

Statistical energy analysis (SEA) is a method for understanding energy transfer paths related to vibration noise generation. In SEA, a target object is separated virtually into subsystems among which the transfer of vibration energy can be quantified. Conventionally, SEA is applied to structures that comprise thin plates, such as the bodies of large ships. The structure is then designed so that the transfer of vibration energy is varied to avoid energy being concentrated on any one subsystem. Although SEA is an effective method for preventing vibration noise problems, it becomes critically inaccurate when applied to structures with low modal density. This paper is aimed at establishing a new measuring method that provides high accuracy for structures with arbitrary modal density. Evaluations of three simplified structures with different modal densities are conducted to determine how to improve the conventional measurement method.

Keywords: Noise, Vibration, SEA, Experimental, Modal Density

I-INCE Classification of Subject Number: 72

1. INTRODUCTION

Finite element analysis (FEA) and experimental modal analysis are typically used to analyze vibration noise in mechanical structures. These methods are effective for relatively low frequencies, at which the modal density also tends to be relatively low, thereby allowing these methods to identify the few modes that are responsible for the vibration. This allows countermeasures to be applied to the nodes and antinodes of the relevant modal vibrations. However, at relatively high frequencies, at which the modal density also tends to be relatively high, many modes are responsible. It then becomes extremely difficult to improve the vibration characteristics by suppressing all the relevant modes.

¹ kazumasa_ikeda@denso.co.jp

² toru@kanagawa-u.ac.jp

Conversely, statistical energy analysis (SEA) [1] is known to be effective for analyzing vibration noise at high frequencies. SEA treats the target object as a group of subsystems and focuses on the power balance among those subsystems. This technique has been applied to large structures that consist of thin panels, including ships and automobiles [2], [3]. SEA enables structural design from a perspective different from that of FEA and experimental modal analysis, which deal with modes, by adjusting the power transferred among the subsystems to prevent vibration noise problems. However, a disadvantage of SEA is that its analytical accuracy degrades at low frequencies, at which the modal density tends to be low. For this reason, SEA is typically not used for low-frequency analysis.

This paper proposes and verifies a high-precision analysis method that applies experimental SEA to block structures whose modal density is lower than that of panel structures.

2. FUNDAMENTAL EQUATIONS OF SEA MODEL

SEA considers the target object as a group of subsystems and focuses on the power balance among those subsystems. If subsystem i is adjacent to subsystem j , then the power balance equation for subsystem i consists of (i) the power P_i input from outside the system, (ii) the dissipation power P_{di} converted into heat inside subsystem i , (iii) the power P_{ij} transferred to the adjacent subsystem j , and (iv) the power P_{ji} transferred from the adjacent subsystem j .

We will consider a system that consists of two structural subsystems as shown in

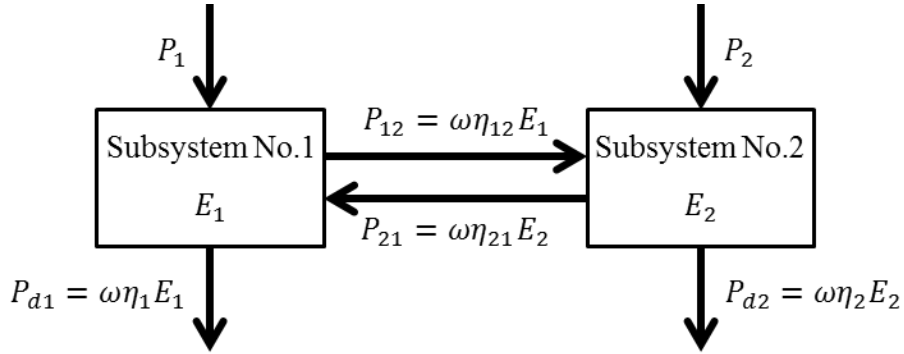


Figure 1: Power balance equations of two subsystems

Fig. 1. The power balance for subsystems 1 and 2 is represented by

$$P_1 = P_{d1} + P_{12} - P_{21}, \quad (1)$$

$$P_2 = P_{d2} + P_{21} - P_{12}. \quad (2)$$

The dissipation power P_{di} is given by Equation 3 using the vibration energy E_i of subsystem i at angular frequency ω :

$$P_{di} = \omega\eta_i E_i, \quad (3)$$

Here, the proportionality factor η_i , known as the internal loss factor (ILF), indicates attenuation in subsystem i . The power P_{ij} transferred from subsystem i to subsystem j is given by

$$P_{ij} = \omega\eta_{ij} E_i, \quad (4)$$

where η_{ij} , known as the coupling loss factor (CLF), is a parameter specific to SEA that quantifies the ease with which energy is transferred between the subsystems. Substituting Equations 3 and 4 into Equations 1 and 2 and rearranging gives

$$\begin{bmatrix} P_1 \\ P_2 \end{bmatrix} = \omega \begin{bmatrix} \eta_1 + \eta_{12} & -\eta_{21} \\ -\eta_{12} & \eta_2 + \eta_{21} \end{bmatrix} \begin{bmatrix} E_1 \\ E_2 \end{bmatrix}, \quad (5)$$

which is rearranged further to give

$$\mathbf{P} = \omega \mathbf{L} \mathbf{E}, \quad (6)$$

where \mathbf{P} is the input power vector, \mathbf{E} is the vibration energy vector, and \mathbf{L} is the loss factor matrix.

3. CONVENTIONAL METHOD

In this section, a model-identification method based on conventional experimental SEA is introduced, and the model accuracy is assessed when three kinds of structures with different modal densities are analyzed by the conventional method. Furthermore, the cause of low accuracy is studied, and we clarify points to improve.

3.1. Identifying a Model Experimentally

In the case of an existing object, the ILFs and CLFs can be calculated by conducting an excitation experiment to measure the input power and the vibration energy. This technique is called experimental SEA. Several methods for obtaining the ILFs and CLFs have been proposed. The power injection method [3] calculates the ILFs and CLFs simultaneously, and the approximated power injection method [4] determines the CLFs by considering only the adjacent subsystems. In the present study, the excitation experiment was conducted based on the approximated power injection method, which excites an arbitrary subsystem and measures the responses of that subsystem and the adjacent subsystems. This process is then conducted on all subsystems to identify the ILFs and CLFs. When a subsystem is excited, the excitation force and acceleration at an excitation point are measured to determine the input power. The acceleration at a response point is then measured to obtain the vibration energy. The input power and the vibration energy of each subsystem are given by

$$P_i = \frac{1}{2} \text{Re}[F \cdot v_{input}] = -\frac{1}{4\pi f} \text{Im}[F \cdot a_{input}], \quad (7)$$

$$E_i = \frac{1}{2} m_i v_i^2 = \frac{m_i}{2\omega^2} \sum_{k=1}^n \frac{a_k a_k^*}{n}. \quad (8)$$

In Equation 7, F is the excitation force, v_{input} is the velocity at the excitation point, a_{input} is the acceleration at the excitation point, and f is the excitation frequency. $\text{Re}[\]$ specifies the real part and $\text{Im}[\]$ the imaginary part. In Equation 8, m_i is the effective mass of subsystem i , v_i is the velocity of subsystem i , a_k is the acceleration response at measurement point k on subsystem i , n is the number of response points per subsystem, and the asterisk specifies the complex conjugate.

Using P_i and E_i from Equations 7 and 8, the ILF η_i and the CLF η_{ij} are determined by

$$\eta_i = \frac{1 - \omega \sum_{j \neq i}^n \left(\frac{\eta_{ij} E_{ii}}{P_i} - \frac{\eta_{ji} E_{ji}}{P_i} \right)}{\omega \frac{E_{ii}}{P_i}}, \quad (9)$$

$$\eta_{ij} = \frac{\frac{E_{ji}}{P_i}}{\omega \frac{E_{ii}}{P_i} \frac{E_{jj}}{P_j}}, \quad (10)$$

where E_{ii} is the vibration energy of subsystem i when that subsystem is excited, and E_{ji} is the vibration energy of subsystem j when subsystem i is excited.

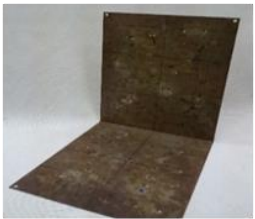

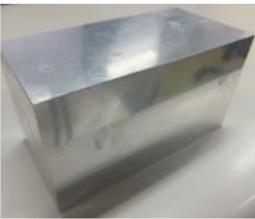
Conventionally, experimental SEA is often used in frequency ranges in which elastic vibration is dominant and the modal density is high [2], [5]. In that frequency range, vibration in the out-of-plane direction becomes dominant on objects whose thickness is less than the planar dimensions [6], [7]. For that reason, the excitation force is loaded in only the out-of-plane direction and the response is measured in only the out-of-plane direction.

By contrast, experimental SEA is almost never used in frequency ranges with low modal density, where the model accuracy is reported to deteriorate. That is the main reason why no examples can be found. One of the main themes of the present paper is to identify the causes for this low model accuracy and realize a way to obtain sufficient accuracy.

3.2. Relationship between Modal Density and Model Accuracy

In this subsection, we determine how the modal density affects the model accuracy. Experimental SEA models are constructed of three kinds of targets with different modal densities as shown in Table 1. The specifications of each target are given in Sections 3.2.1, 3.2.2, and 3.2.3.

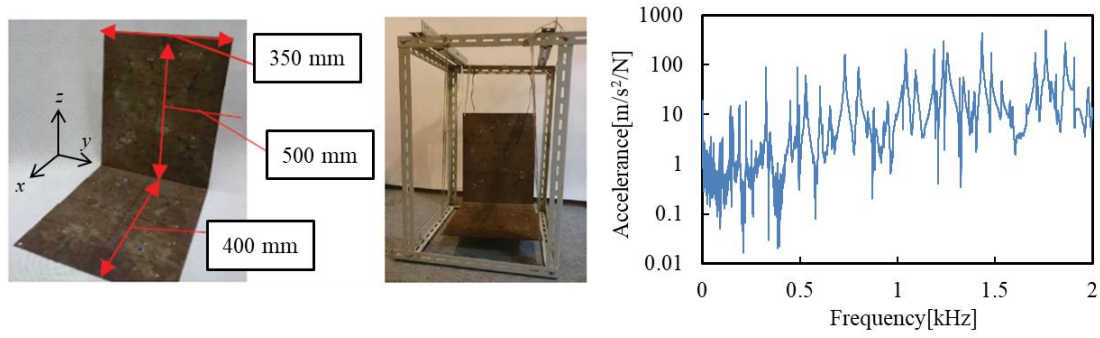
Table 1. Example structures with different modal densities

Modal density	High	Middle	Low
Test Structure			
Designation	L-shaped structure	Hollow structure	Solid-core structure

3.2.1. L-shaped Structure

The first example is an L-shaped structure that is made of steel and comprises two crossed planes as shown in Fig. 2(a). The structure is supported by strings as shown in Fig. 2(b), and frequency response function shown in Fig. 2(c) was obtained from a hammering test. There are more than 40 modes in the range 0–2 kHz, giving a modal density greater than 20/kHz.

We assess the model accuracy of the conventional experimental SEA method for this structure. As shown in Fig. 3(a), the model is taken to have two subsystems that are connected at the bending part. Excitation points and response points are located at the center of each subsystem. Excitation is applied in the out-of-plane direction and the response is measured in the out-of-plane direction. With the excitation force F , the accelerance a_{input} of the excitation point, and the accelerance a_k of the response point all obtained from the excitation experiment, the ILF η_i of each subsystem and the CLF η_{ij} between the two subsystems are identified using Equations 7–10. Using η_i , η_{ij} , and the input power P_i , the predicted vibration energy can be obtained. Meanwhile, using F , a_{input} , a_k , and Equation 8, the measured vibration energy can be obtained. The more precisely

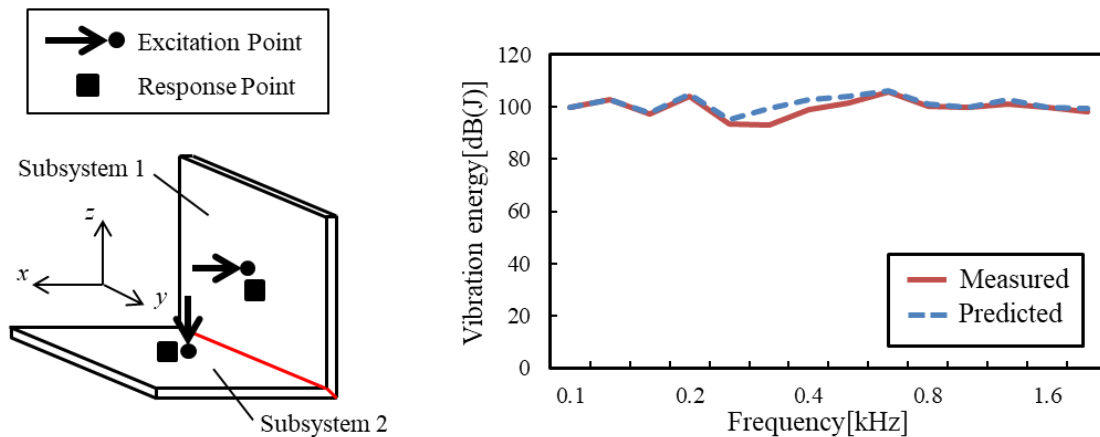


(a) Overview (b) Boundary condition (c) Frequency response function

Figure 2: L-shaped structure

we can identify η_i and η_{ij} , the less the error between the predicted and measured vibration energies.

The results of the predicted and measured vibration energies are shown in Fig. 3(b). The two energies agree with each other below 2 kHz, with the largest error being approximately 5 dB at 0.315 kHz. We can therefore conduct this level of model identification using the conventional experimental SEA method.



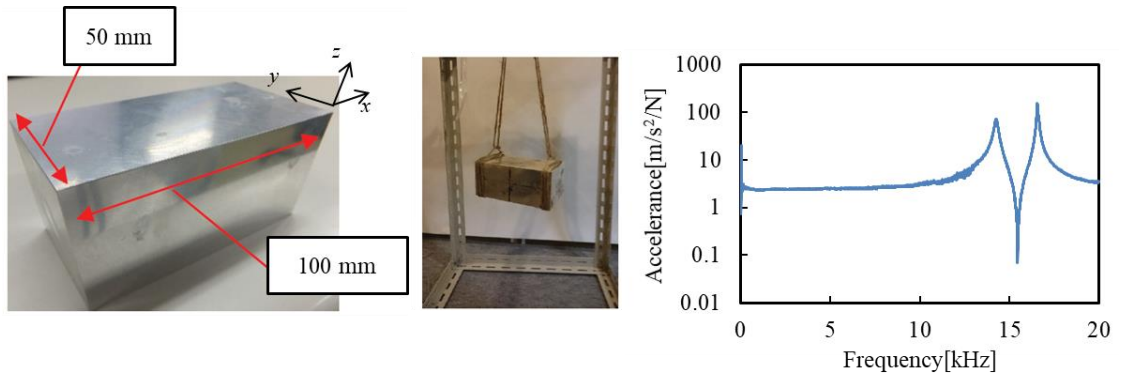
(a) Subsystems (b) Measured and predicted vibration energies

Figure 3: Statistical energy analysis (SEA) data for L-shaped structure

3.2.2. Solid-core Structure

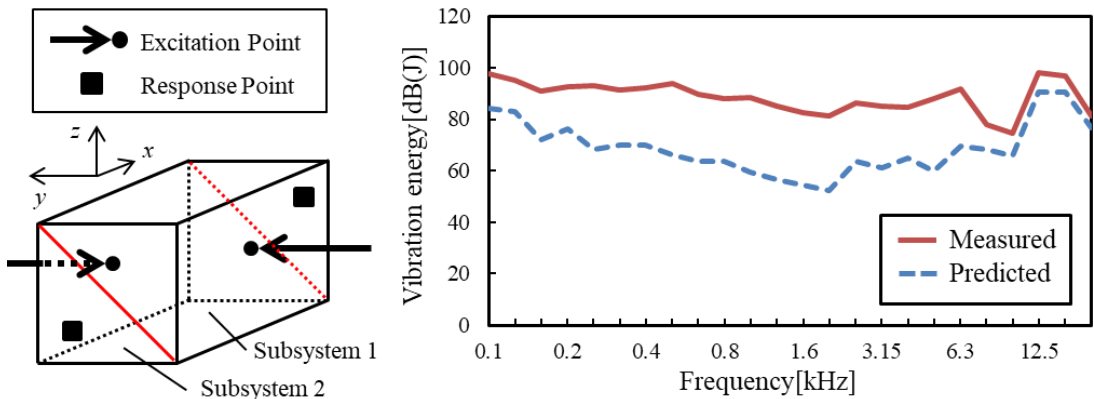
The second example is a solid-core structure made of aluminium as shown in Fig. 4(a). The structure is supported by strings as shown in Fig. 4(b), and frequency response function shown in Fig. 4(c) was obtained from a hammering test. There are no modes below 14 kHz, which is the first resonance frequency, so the modal density is zero.

We assess the model accuracy of the conventional experimental SEA method for this structure. As shown in Fig. 5(a), the model is taken to have two subsystems that are divided by the diagonal line. Excitation points are located at the center of each subsystem, and response points are located on the edge of each subsystem. Excitation is applied in the out-of-plane direction and the response is measured in the out-of-plane direction. The results for the predicted and measured vibration energies are shown in Fig. 5(b). There is now a large error at every frequency, particularly below 6.3 kHz, where the error exceeds 20 dB error. It is therefore unrealistic to apply the conventional method in this case, and improvement is needed to conduct precise model identification.



(a) Overview (b) Boundary condition (c) Frequency response function

Figure 4: Solid-core structure

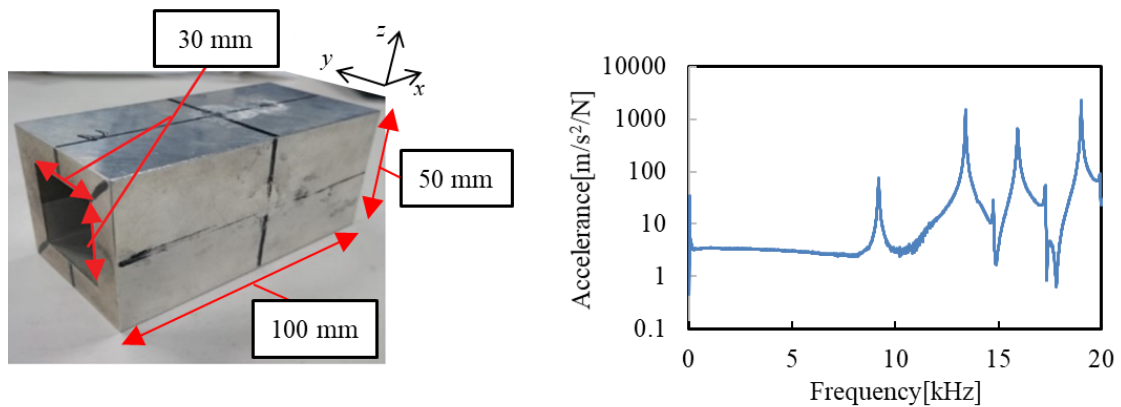


(a) Subsystem (b) Measured and predicted vibration energies

Figure 5: SEA data for solid-core structure

3.2.3. Hollow Structure

The third example is a hollow structure made of aluminium as shown in Fig. 6(a). The structure is supported by strings like the solid-core structure in Fig. 4(b), and the frequency response function shown in Fig. 6(b) was obtained from a hammering test. There are no modes below 9 kHz, which is the first resonance frequency, so rigid-body movement is dominant in that frequency range. Otherwise, there are five modes in the range 10–20 kHz, giving a modal density of 0.5/kHz in that range.



(a) Overview (b) Frequency response function

Figure 6: Condition of hollow structure

We assess the model accuracy of the conventional experimental SEA method for this structure. As shown in Fig. 7(a), the model is taken to have two subsystems that are divided by the diagonal line as with the solid-core structure. Excitation points are located at the center of each subsystem, and response points are located on the edge of each subsystem. Excitation is applied in the out-of-plane direction and the response is measured in the out-of-plane direction. The results for the predicted and measured vibration energies are shown in Fig. 7(b). There is again a large error at every frequency, particularly below 10 kHz, where the error is approximately 20 dB. It is therefore unrealistic to apply the conventional method in this case also, and improvement is again needed to conduct precise model identification.

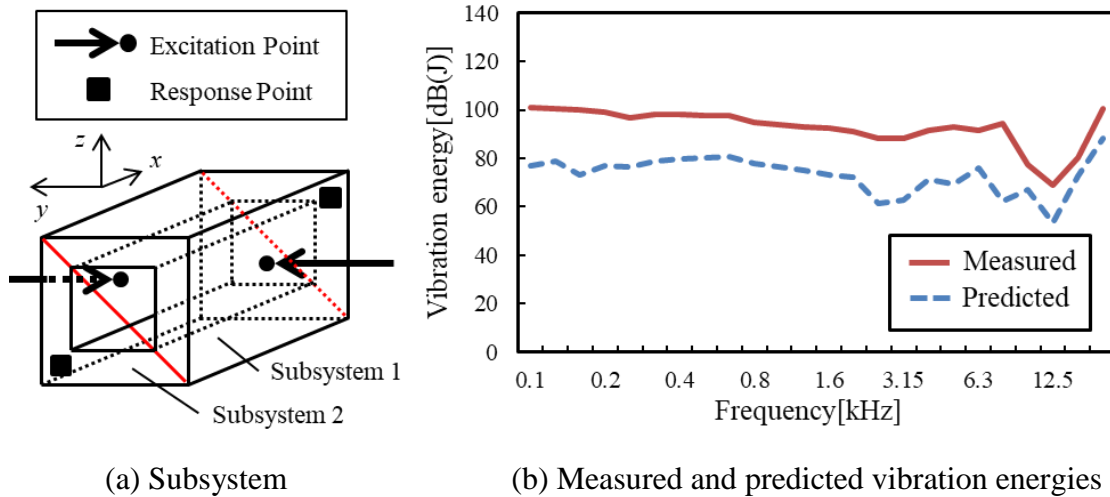


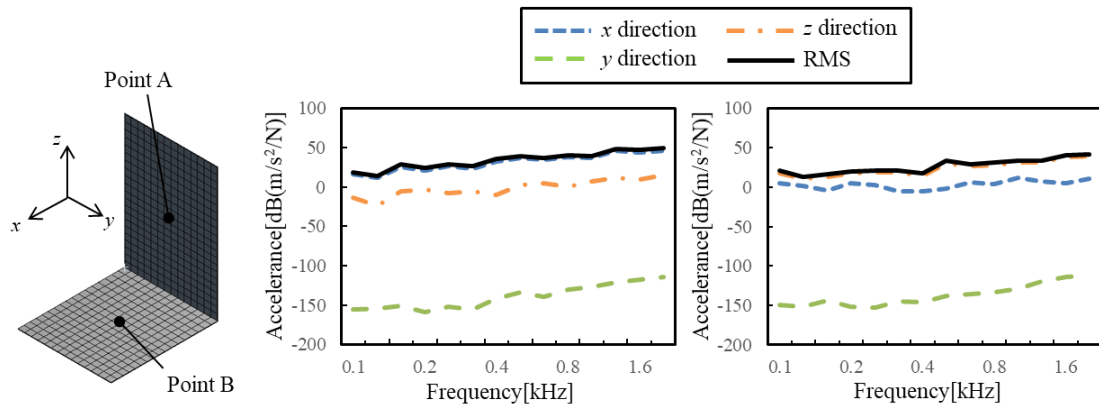
Figure 7: SEA data for hollow structure

3.3. Effect of Modal Density on Vibration Behavior

As shown above, in contrast to the L-shaped structure with its high modal density, the model accuracy is low for both the solid-core structure and the hollow structure with their low modal densities. To investigate the reason for this, we analyzed the vibration behavior of each structure using the general-purpose FEA software ANSYS 18.2 (ANSYS Inc.).

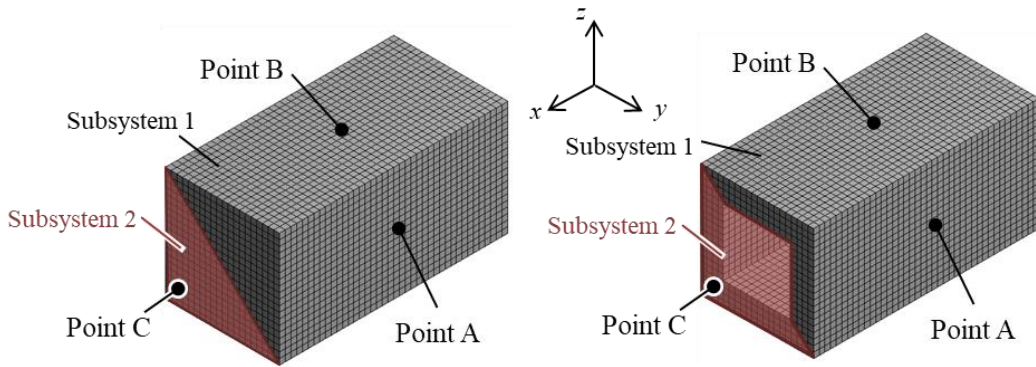
First, we consider the vibration behavior of the L-shaped structure, which contains many modes in the frequency range 0–2 kHz, as shown in Fig. 2(c). The FEA model of this structure is shown in Fig. 8(a). The accelerances of points A (center of subsystem 1) and B (center of subsystem 2) were calculated when an excitation force of 1 N was applied to point A in the x (out-of-plane) direction. The accelerances are shown in Fig. 8(b) and (c), where the blue short-dash line is the accelerance in the x direction, the green long-dash line is that in the y direction, the orange dot-dash line is that in the z direction, and the solid black line is the root-mean-square (RMS) accelerance of the three orthogonal directions. For points A and B, the accelerances in the x and z directions, respectively, are both nearly equal to the RMS. The results indicate that the vibration energy can be obtained from the accelerance in the out-of-plane direction, corresponding to the result in Fig. 3(b) that the measured and predicted vibration energies agree with each other.

Next, we consider the vibration behaviors of the solid-core and hollow structures, whose FEA models are shown in Fig. 9. The accelerances of points A (center of the xz plane of subsystem 1), B (center of xy plane of subsystem 2), and C (edge of the yz plane of subsystem 2) were calculated when an excitation force of 1 N was applied to point A



(a) FEA model (b) Accelerance of point A (c) Accelerance of point B

Figure 8: Accelerance of the L-shaped structure in each direction as calculated by finite element analysis (FEA)

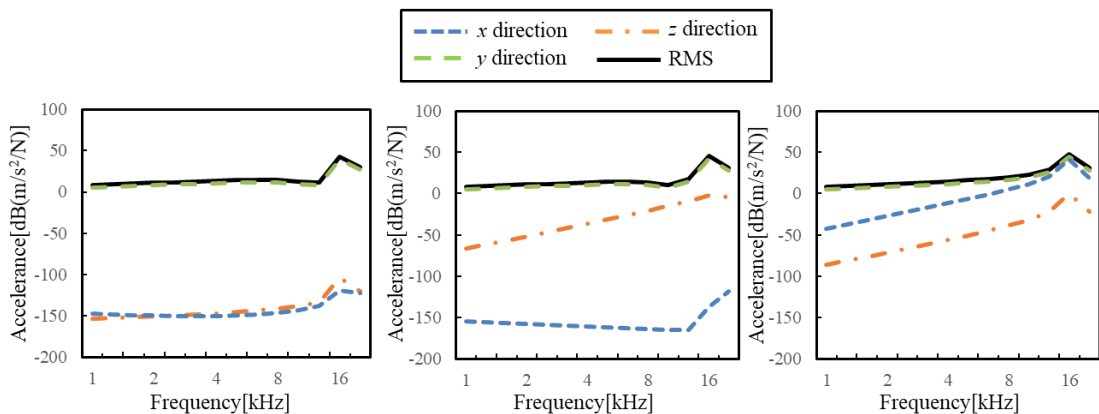


(a) FEA model of solid-core structure (b) FEA model of hollow structure

Figure 9: FEA models of the solid-core and hollow structures

in the y (out-of-plane) direction. The results for the solid-core structure are shown in Fig. 10, and those for the hollow structure are shown in Fig. 11; the lines have the same meanings as in Fig. 8.

At low frequency, the accelerance of point A in the y (out-of-plane) direction is nearly equal to the RMS, but the accelerances of points B and C in the z and x (out-of-plane) directions are both far from the RMS. However, the fact that the accelerance of each response point in the y excitation direction is nearly equal to the RMS makes the y



(a) Point A (b) Point B (c) Point C

Figure 10: Accelerance of the solid-core structure in each direction

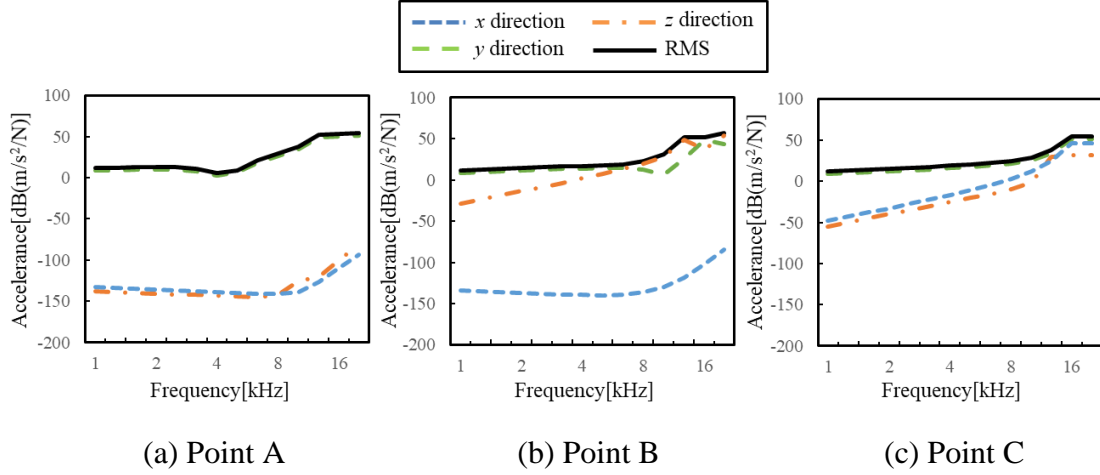


Figure 11: Accelerance of the hollow structure in each direction

direction the dominant one. Nevertheless, the accelerances of points B and C in the x and z directions increase at higher, in some cases exceeding that in the y direction. Furthermore, the distinction between low and high frequency is at 12.5 kHz in the case of the solid-core structure and at 8 kHz in the case of the hollow structure. For both structures, this separating value also distinguishes between the frequency range in which there are no modes and the one in which there are scattered modes, as shown in Figs. 4(c) and 6(c). Therefore, calculating the vibration energy requires (i) only the accelerance in the excitation direction in the no-mode frequency range and (ii) the accelerances in all three orthogonal directions in the scattered-mode frequency range.

4. PROPOSED METHOD

Thus far, we have clarified various points regarding how to conduct precise model identification for three structures with different modal densities. In this section, we assess the effectiveness of a new method for conducting precise model identification.

4.1. Perspective and Method of Improvement

To improve the model accuracy, we consider how experimental SEA acts in three types of frequency range with different vibration behaviors, namely (i) a frequency range in which there are clusters of modes (e.g., the 0–2 kHz range for the L-shaped structure), (ii) a no-mode frequency range (e.g., the 0–14 kHz range for the solid-core structure and the 0–9 kHz range for the hollow structure), and (iii) a scattered-modes frequency range (e.g., the 14–20 kHz range for the solid-core structure and the 9–20 kHz range for the hollow structure).

In frequency range (i), the accelerance in the out-of-plane direction is much larger than those in the in-plane directions and nearly equal to the RMS of accelerances in all three orthogonal directions. Consequently, to obtain the vibration energy precisely, it is sufficient to measure only the accelerance in the out-of-plane direction. That is the conventional method discussed in Section 3.1.

In frequency range (ii), the accelerance in the excitation direction becomes nearly equal to the RMS of accelerances in all three orthogonal directions. Consequently, to obtain the vibration energy precisely, it is sufficient to measure only the accelerance in the excitation direction.

In frequency range (iii), because the accelerance shows large values randomly in each direction, we must measure the accelerances in all three orthogonal directions to obtain the vibration energy precisely.

The effectiveness of the improved method is assessed in Sections 4.2 and 4.3 for frequency ranges (ii) and (iii), respectively. Because changing the excitation points and response points would change the vibration energy, we assess the improved method using the same points as those used to assess the conventional method.

4.2. Validation in No-Mode Frequency Range

In a no-mode frequency range, the proposed method for obtaining the vibration energy precisely involves only the accelerance in the excitation direction. Here, validation is performed using the solid-core structure and the hollow structure.

The solid-core structure and hollow structure are subjected to model identification as in Sections 3.2.2 and 3.2.3. Here, we measure only the accelerance in the y direction, namely the excitation direction. The measured and predicted vibration energies are shown in Fig. 12. Here, we introduce a calculation method that accounts for the influence of rigid-body movement [8]. For both structures, the accuracy is high in the relevant no-mode frequency range, thereby confirming that measuring in only the excitation direction is effective for obtaining the vibration energy precisely in a no-mode frequency range.

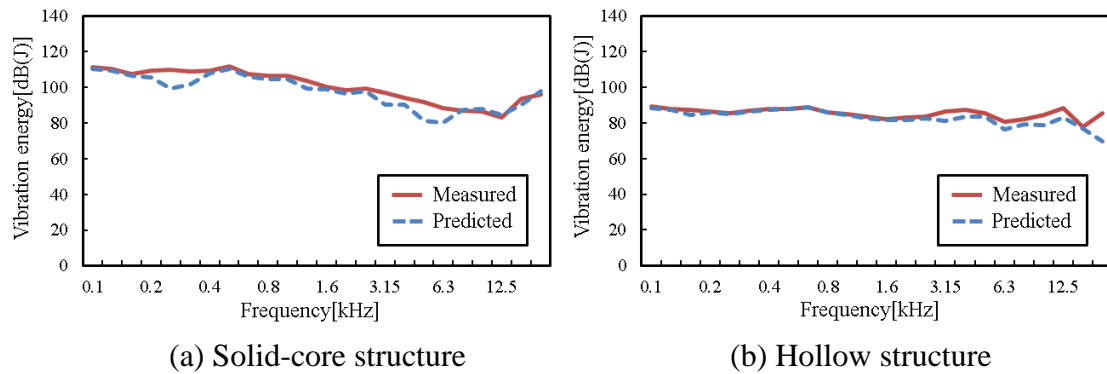


Figure 12: Measured vibration energy (solid red line) of each structure compared with that predicted by applying unidirectional excitation and then measuring the response in the excitation direction (dashed blue line)

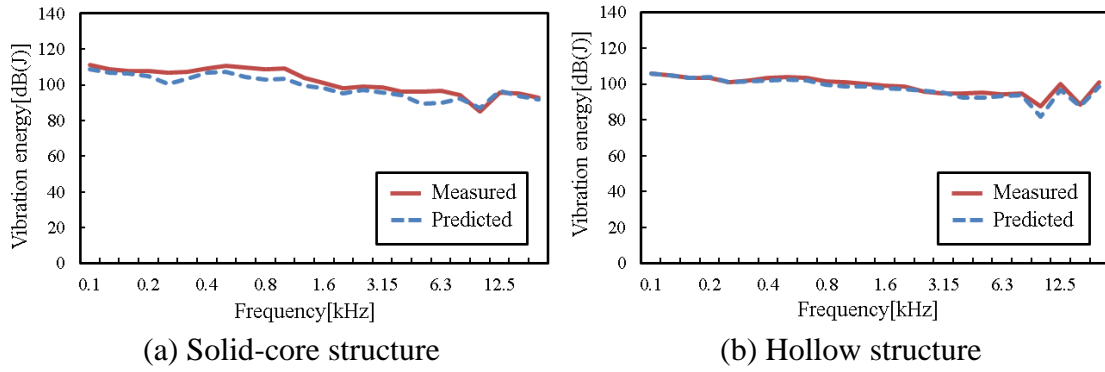
4.3. Validation in Scattered-modes Frequency Range

The proposed method for obtaining the vibration energy precisely in a scattered-modes frequency range involves determining the accelerances in all three orthogonal directions. Here, validation is done using the solid-core structure and the hollow structure.

The solid-core structure and hollow structure were subjected to model identification as in Sections 3.2.2 and 3.2.3. Here, we measure the accelerances in the x , y , and z directions, and the measured and predicted vibration energies are shown in Fig. 13. For both structures, the accuracy is high in the relevant scattered-modes frequency range, thereby confirming that measuring in all three orthogonal directions is effective for obtaining the vibration energy precisely in a scattered-modes frequency range.

4.4. Unified Method for All Frequency Ranges

Thus far, we have confirmed that (i) the conventional method of measuring the accelerance in the out-of-plane direction is effective in a frequency range in which there are clusters of modes, (ii) the proposed method of measuring the accelerance in the excitation direction is effective in a no-mode frequency range, and (iii) the other newly proposed method of measuring the accelerance in all three orthogonal directions is effective in a scattered-modes frequency range. However, the fact that the choice of



(a) Solid-core structure (b) Hollow structure
Figure 13: Measured vibration energy (solid red line) of each structure compared with that predicted by applying excitations and then measuring the responses in all three orthogonal directions (dashed blue line)

measuring direction depends on the frequency range means that the modal density must be determined and the frequency range of the target object must be assessed in advance. Therefore, a unified method is required that can be used for all frequency ranges.

The conventional method and the two proposed methods are all based on the idea that the measuring direction should be the one that contributes most to the vibration energy. Therefore, the accelerances in the other directions are much smaller. Here, the three orthogonal directions in which measurements are made in a frequency range that has scattered modes include the out-of-plane direction and the excitation direction. We therefore reason that the method of measuring in all three orthogonal directions can be applied with high accuracy to both a no-mode frequency range and a frequency range in which there are clusters of modes. For a no-mode frequency range, this method gives precise model identification, as already shown in Fig. 13. For a frequency range in which there are clusters of modes, the method was applied to the L-shaped structure in an additional experiment, and the results are shown in Fig. 14. The vibration energies agreed reasonably over the entire frequency range, meaning that the method is also applicable to a frequency range in which there are clusters of modes. The method of measuring the accelerances in all three orthogonal directions is therefore applicable to all frequency ranges.

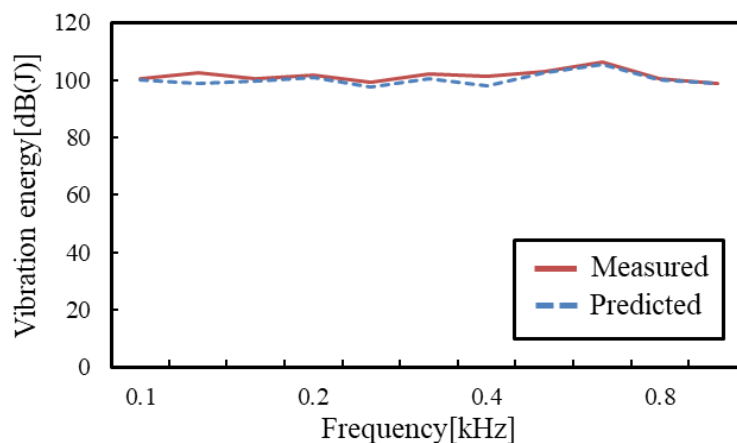


Figure 14: Measured vibration energy (solid red line) of the L-shaped structure and that predicted by applying excitations and then measuring the responses in all three orthogonal directions (dashed blue line)

5. CONCLUSIONS

The conventional opinion of experimental SEA is that its model accuracy is critically poor in frequency ranges with low modal density. In the present study, we analyzed the vibration behaviors of three different structures and found that both the vibration behavior and the appropriate method for measuring the vibration differed according to the frequency range, as explained below. However, the newly proposed method of measuring the accelerances in all three orthogonal directions gives sufficient accuracy in all frequency ranges.

1) In a frequency range in which there are clusters of modes, the accelerance in the out-of-plane direction makes the main contribution to the vibration energy. Highly accurate model identification can therefore be conducted by measuring only the accelerance in the out-of-plane direction.

2) In a no-mode frequency range, the accelerance in the excitation direction makes the main contribution to the vibration energy. Highly accurate model identification can therefore be conducted by measuring only the accelerance in the excitation direction.

3) In a scattered-modes frequency range, the accelerances in all three orthogonal directions influence the vibration energy. Highly accurate model identification can therefore be conducted by measuring the accelerances in all three orthogonal directions.

6. REFERENCES

1. R. H. Lyon, “*Statistical Energy Analysis of Dynamical Systems*”, Theory and Applications, MIT Press, (1975)
2. T. Miyahara, T. Yamazaki, M. Kamata, “*Vibration Analysis for a White Body of Automotive Vehicle Using Predictive SEA*”, Dynamics and Design Conference, (2002)
3. D. A. Bies, S. Hamid, “*In situ determination of loss and coupling loss factors by the power injection method*”, Journal of Sound and Vibration Volume 70, Issue 2, (1980), pp. 187-204
4. N. Lalor, “*Practical Considerations for the Measurement of Internal and Coupling Loss Factors on Complex Structures*”, ISVR Technical Report, No.182, (1990)
5. T. Yamazaki, K. Kuroda, A. Mori, “*A Structural Design Process for Reducing Structure-Borne Sound on Machinery Using SEA*”, Vol. 73, No. 726, (2007)
6. R. H. Lyon, “*In-plane Contribution to Structural Noise Transmission*”, Noise Control Engineering Journal, 26, 1, (1986), pp. 22-27
7. K. Kuroda, T. Yamazaki, F. Kuratani, “*Influence of In-Plane Vibration on SEA Model for Flexural Vibration on Plate Structures*”, Vol. 74, No. 744, (2008)
8. K. Ando, Y. Matsumura, Y. Ito, H. Nakamura, T. Yamazaki, K. Ikeda, “*Discussion on experimental SEA modelling of structures with low modal density*”, Dynamics and Design Conference, (2015)